MODELING AND SIMULATION OF STRESS FOR CEMENTED CARBIDE CYLINDRICAL END MILL

WU Qiong[(a)], Li Da Peng[(b)]

State Key Lab of Virtual Reality Technology and Systems, School of Mechanical Engineering and Automation, Beihang University, Beijing 100191, China

[(a)]wuqiong@buaa.edu.cn [(b)] lidapeng925@163.com

ABSTRACT

The cutting force and stress of tool is important factor for failure of tool in the cutting process. Predictions of the forces and stress in milling are often needed in order to establish automation or optimization of the machining processes. A theoretical model for milling forces according to a predictive machining theory and the experiment of milling has been presented. The action of a milling cutter is considered as the simultaneous work of a number of single-point cutting tools, and milling forces are predicted from input data of the workpiece material properties, the cutter parameters and tooth geometry, and the cutting condition. Based on cutting force model, the stress of cemented carbide cylindrical end mill is developed. The numerical simulation and the experiment are performed to compare with stress model of mill. Milling tool stress experimental tests and numerical simulation separately were conducted to verify the simulation. The study provides a reliable method for analyzing stress of tool in the milling process.

Keywords: simulation; modeling; finite element analysis; milling

1. INTRODUCTION

Milling is widely used in many areas of manufacturing. During the cutting operation, cutters may break down either at the shank of cutter or at the tip of cutter. Some operation may occur on both conditions. Investigation of failure requires not only knowledge of the state of stress but also failure criteria. The literatures (Kurt, 2009; Jemal, 1992).shows the stresses for metal cutting, it is observed that the analytical method, the finite element method (FEM) and Artificial Neutral Network (ANN), the mathematical modeling method were used in order to analyze the stresses of the orthogonal cutting tools, the cutters for turning and the end mill. Then the experimental stress analysis was used to verify the stress results obtained by FEM, ANN or the analytical method (Kurt, 2009). The orthogonal cutting tool has two types of premature failure: brittle failure, such as edge fracture and edge chipping, and ductile failure, such as edge plastic deformation was discussed by Zhou, Andersson and Stahl (1997).

The estimation of cutting force is an important factor to predict the cutting tool stresses. Some researchers used a series of experimental measurements in order to find the cutting forces (Kumar, Mohan, Rajadurai and Dinakar, 2003; Wu, Zhang and Zhang, 2009). Some researchers presented the analytical cutting force model (Budak, Altintas, and Armarego, 1996). The experimental stress analysis method are the electrical-resistance strain gage and its associated instrumentation, transmission and reflection photo-elasticity, brittle coating, Moiré gratings, Moiré interferometry, x-ray diffraction, holographic and laser speckle interferometry and thermo-elastic stress analysis. From these methods, the electrical-resistance strain gages are widely used in experimental stress analysis (Tsai, 2007). The strain gages have been used to study the deflection and residual stress of the end mill (Kops and Vo, 1990; Rendler and Vigness, 1966).

In this paper, the cutting forces will be analytically predicted using the cutting force formulas. The maximum principal stress, the maximum shear stress and von Mises stress will be investigated by means of FEM commercial software (MSC Patran/Nastran). These results are verified with the results obtained from the electrical-resistance strain gage.

2. MILLING FORCE MODEL

The cutting forces based on the analytical theory(L. Kops and D. T. Vo 1990) are used to investigate the deflection and stresses in the end mill. Tangential ($dF_{t,j}$), radial ($dF_{r,j}$), and axial ($dF_{a,j}$) , forces acting on a differential flute element with height dz are expressed in Eq.(1).

$$\begin{aligned} dF_{t,j}(\phi,z) &= \lfloor K_{tc}h_j(\phi_j(z)) + K_{te} \rfloor dz, \\ dF_{r,j}(\phi,z) &= \left[K_{rc}h_j(\phi_j(z)) + K_{re} \right] dz, \\ dF_{a,j}(\phi,z) &= \left[K_{ac}h_j(\phi_j(z)) + K_{ae} \right] dz. \end{aligned} \quad (1)$$

dF_t, dF_r, dF_a ——Differential tangential, radial and axial forces;

K_{tc}, K_{rc}, K_{ac} ——Shear force coefficients in tangential, radial and axial directions;

K_{te}, K_{re}, K_{ae} ——Cutting force coefficients in the tangential, radial and axial directions;

ϕ —— Rotation angle of the milling cutter;

z —— Height of axial directions

$h(\phi, z)$ ——Chip thickness specified by ϕ , z;

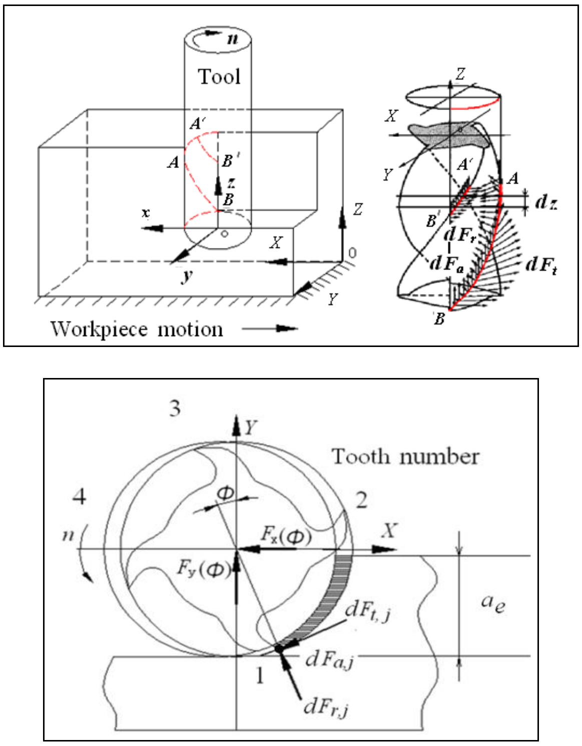

Figure 1: Model of milling force

The elemental forces are resolved into feed (x), normal (y), axial (z) directions using the transformation

$$
\begin{aligned}
dF_{x,j}\ \phi_j(z) &= -dF_{t,j}\cos\phi_j(z) - dF_{r,j}\sin\phi_j(z),\\
dF_{y,j}\ \phi_j(z) &= +dF_{t,j}\sin\phi_j(z) - dF_{r,j}\cos\phi_j(z),\\
dF_{z,j}\ \phi_j(z) &= +dF_{a,j}.
\end{aligned}
\tag{2}
$$

The average cutting forces are

$$
\left.
\begin{aligned}
\bar{F}_x &= \left\{\frac{Nac}{8\pi}\,K_{tc}\cos 2\phi - K_{rc}(2\phi-\sin 2\phi) \quad + \frac{Na}{2\pi}[-K_{te}\sin\phi + K_{re}\cos\phi]\right\}_{\phi_{st}}^{\phi_{ex}}\\
\bar{F}_y &= \left\{\frac{Nac}{8\pi}\,K_{tc}(2\phi-\sin 2\phi) + K_{rc}\cos 2\phi \quad - \frac{Na}{2\pi}[K_{te}\cos\phi + K_{re}\sin\phi]\right\}_{\phi_{st}}^{\phi_{ex}}\\
\bar{F}_z &= \frac{Na}{2\pi}[-K_{ac}c\cos\phi + K_{ae}\phi]_{\phi_{st}}^{\phi_{ex}}
\end{aligned}
\right\}
\tag{3}
$$

β ——Helix angle;

a_e —— radial depth of cut

N —— number of teeth

ϕ_{st} —— start angle

ϕ_{ex} —— exit angle

X, Y, Z—— Global stationary coordinate system

3. MILLING FORCE TEST PROCESS

It is assumed that the edge force coefficients (K_{te} , K_{re} and K_{ae}) are constant and have little effect on the resultant forces. By means of Eq. (3), the milling forces are obtained by measuring cutting force device as shown in Figure 2. The parameters of cutting process is shown in Tab.1.

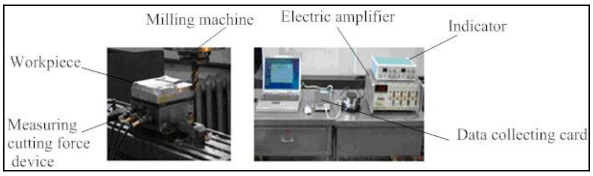

Figure 2 Set Up of Milling Force Test Process

Table 1: Parameters of Cutting Process

Parameters name (unit)	Value	Parameters name (unit)	Value
Rotation speed r/min	3000	Material of tool	Hard alloy
Feed speed mm/min	400	Number of tooth	2
Depth of cutting mm	2	Helical angle	20
Width of cutting mm	6	Length of cantilever mm	120
Material of workpiece	7075	Outer Diameter mm	12
Hardness HRA	90	Rake angle °	20

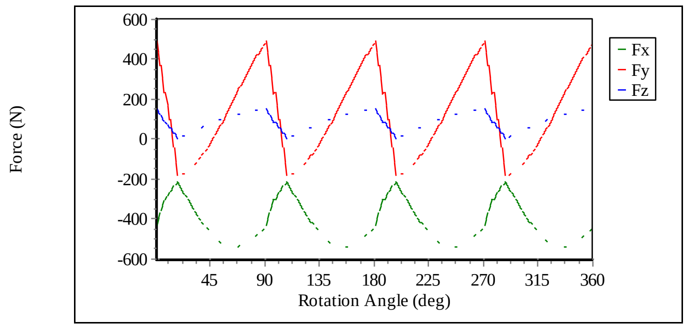

Figure 3: Cutting Force in 360° Rotation Angle

Based on cutting force experimental results as shown in Figure 3, the average cutting forces per tooth can easily be calculated. The milling force coefficients (N/mm^2) of 7075 aluminum alloy were obtained to

$$K_{rc} = 893.3,\ K_{tc} = 1880.0,\ K_{ac} = 157.1.$$

Apply these coefficients for Eq. (3) to get the milling force model

4. STRESS ANALYSIS OF MILLING MODEL

The shape of the cutter edge as described in Figure 4 (a) is assumed as a semi-infinite wedge .The thickness of the wedge is taken as unity, so *P* or *F* is the load per unit thickness acting at the vertex of a very large or semi-infinite wedge as shown Figure 4 (b).

Assuming that the stress function for *y*-direction is

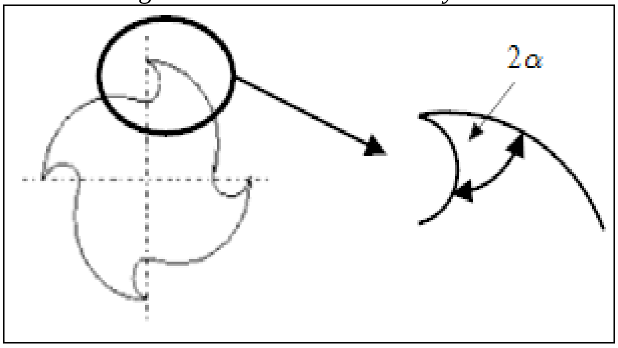

(a) Description of Cutter Edge

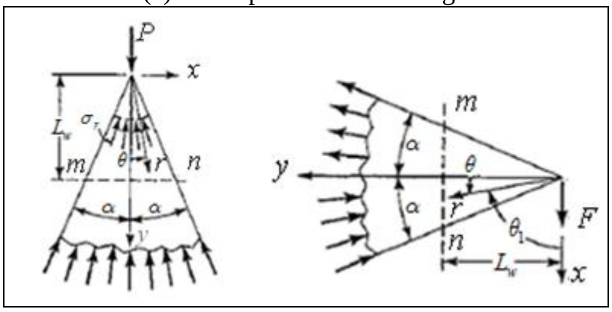

(b) Cutter Edge or Pivot (c) Wedge Cantilever

Figure 4: Description of Cutter Edge and Wedge of Unit Thickness Subjected of Concented Cutting Load

$$\psi = kPr\theta\sin\theta \tag{4}$$

The corresponding stress components are obtained by the following relations.

$$\sigma_r = \frac{1}{r}\frac{\partial\psi}{\partial r} + \frac{1}{r^2}\frac{\partial^2\psi}{\partial\theta^2} \tag{5}$$

$$\sigma_\theta = \frac{\partial^2\psi}{\partial r^2} \tag{6}$$

$$\tau_{r\theta} = -\frac{\partial}{\partial r}\left(\frac{1}{r}\frac{\partial\psi}{\partial\theta}\right) \tag{7}$$

By substituting Eq. (4) into Eq.(5) to (7), the radial stresses are :

$$\sigma_r = 2kP\frac{\cos\theta}{r}\,,\ \ \sigma_\theta = 0\,,\ \tau_{r\theta} = 0 \tag{8}$$

The constant *k* can be obtained by using the equilibrium condition at the point O. The force resultant action on a cylindrical surface of small radius, shown by the dotted line in Figure 39 (a), must balance *P*. Since The boundary conditions are expressed by

$$\sigma_\theta = 0\,,\ \tau_{r\theta} = 0\,,\ \theta = \pm\alpha \tag{9}$$

$$2\int_0^\alpha (\sigma_r\cos\theta)rd\theta = -P \tag{10}$$

By substituting σ_r in Eq. (5) to Eq. (10)

$$4kP\int_0^\alpha \cos^2\theta d\theta = -P \tag{11}$$

Integration and solving Eq.(11), the constant *k* can be written as

$$k = -\frac{1}{(2\alpha + \sin 2\alpha)} \tag{12}$$

The stress distribution in the edge is therefore

$$\sigma_r = -\frac{P\cos\theta}{r(\alpha + \frac{1}{2}\sin 2\alpha)}\,,\ \sigma_\theta = 0\,,\ \ \tau_{r\theta} = 0 \tag{13}$$

The normal and shearing stresses can be expressed as

$$\sigma_x = \sigma_r\cos^2\theta = -\frac{P\cos^3\theta}{r(\alpha + \frac{1}{2}\sin 2\alpha)} \tag{14}$$

$$\sigma_y = \sigma_r\sin^2\theta = -\frac{P\sin^2\theta\cos\theta}{r(\alpha + \frac{1}{2}\sin 2\alpha)} \tag{15}$$

$$\tau_{xy} = \sigma_r\sin\theta\cos\theta = -\frac{P\sin\theta\cos^2\theta}{r(\alpha + \frac{1}{2}\sin 2\alpha)} \tag{16}$$

By assuming the stress function for *x*-direction

$$\phi = kFr\theta_1\sin\theta_1 \tag{17}$$

Where θ_1 is measured from the line of action of the force. The equilibrium condition is

$$\int_{\frac{\pi}{2}-\alpha}^{\frac{\pi}{2}+\alpha}(\sigma_r\cos\theta_1)rd\theta_1 = 2kF\int_{\frac{\pi}{2}-\alpha}^{\frac{\pi}{2}+\alpha}\cos^2\theta_1 d\theta_1 = -F \tag{18}$$

After integration

$$k = -\frac{1}{(2\alpha - \sin 2\alpha)} \tag{19}$$

By replacing : $\theta_1 = 90 - \theta$

$$\sigma_r = -\frac{F\cos\theta_1}{r(\alpha - \frac{1}{2}\sin 2\alpha)} = -\frac{F\sin\theta}{r(\alpha - \frac{1}{2}\sin 2\alpha)},$$

$$\sigma_\theta = 0,\ \tau_{r\theta} = 0 \tag{20}$$

$$\sigma_x = \sigma_r \cos^2\theta = -\frac{F\sin\theta\cos^2\theta}{r(\alpha - \frac{1}{2}\sin 2\alpha)} \tag{21}$$

$$\sigma_y = \sigma_r \sin^2\theta = -\frac{F\sin^3\theta}{r(\alpha - \frac{1}{2}\sin 2\alpha)} \tag{22}$$

$$\tau_{xy} = \sigma_r \sin\theta\cos\theta = -\frac{F\sin^2\theta\cos\theta}{r(\alpha - \frac{1}{2}\sin 2\alpha)} \tag{23}$$

5. STRESS ANALYSIS AND EXPERIMENT

In order to analyze the stresses and deflection of the milling cutter, the cutter model is built by Unigraphics (UG) software. Then the model is imported to MSC Patran/Nastran software and divided into 4-noded tetrahedral elements. And the fixed boundary condition and the concentrated loads are applied to the model as described in Figure 5 The isotropic material properties are input according to cutter material from Tab.4. The solution type is chosen as “Linear statics” from structural analysis. The elemental cutting forces used are at 37.2° immersion angle. The distribution of Von Mises stresses in Figure 5 (b). The maximum stress occurs at the cutter edge within the loading region. The location of maximum shank stress can decide from these figures. In addition, the values and locations of maximum and minimum stress for the whole cutter can be obtained.

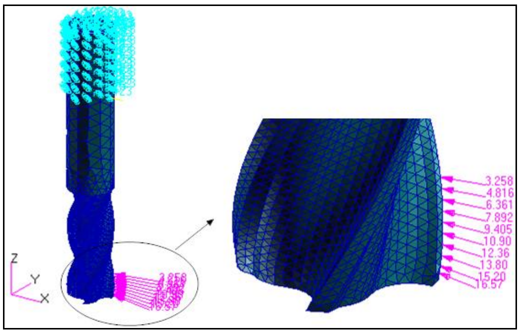

Figure 5(a): Milling Model with FEM Mesh

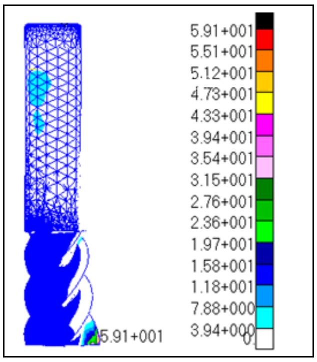

Figure 5(b): Stress Distribution of Cutters

Figure 6 shows equipment used in experiment test to measure strain with electrical-resistance strain gage. The electrical resistance strain gage used in this test is

Figure 6 shows equipment used in experiment test to measure strain with electrical-resistance strain gage. The electrical resistance strain gage used in this test is uniaxial strain gage with 120Ω. The gage factors are 2 and 2.08 for two different size of strain gage. Adhesive is cyanoacrylate. The followings are procedures of strain gage installation.

Figure 6: Set up of Experiment

Before the strain gage is bonded a specified site, its resistance should be measured with multitester. If the resistance is not reached 120Ω, it cannot work correctly. Two terminals of strain gage is connected to a piece of wire with proper length by using electronic soldering iron gun tool and tin lead alloy soldering rosin wire reel. The soldered place must be covered with masking tape to prevent possible damage and environment effects. The strain gage bonding site must be cleaned and the strain gage bonding position should be marked. A drop of adhesive is applied to the back of the strain gage and immediately put the strain gage on the bonding site. The strain gage is covered with an appropriate thing and strongly pressed with a thumb for approximately 1 minute. The two terminals of wire are connected to the strain gage indicator. The value of strain in the strain gage is set to zero. Gage factor will be changed to the value of corresponding material of strain gage. The exciter is moved to touch the cutter and up to desired force. The value of force can be read on force indicator. Value of strain on strain gage indicator is changing according to the given force. When the desired force reaches, strain can be read on strain gage indicator. From experiment the results can be obtain as shown in Table.2

Table.2: Parameters of Cutter Strain of Different Directions between Edge and Shank

Force (N)	Cutter strain on shank			Cutter strain at edge		
	ε_a 180°	ε_b 215°	ε_c 265°	ε_a 60°	ε_b 90°	ε_c 195°
50	-7	4	25	19	2	-137
100	-12	7	46	49	6	-270
150	-19	11	70	78	10	-400
200	-25	14	91	87	14	-550
250	-32	18	115	116	18	-685
300	-37	22	139	145	22	-826
350	-44	26	162	174	26	-960
400	-47	30	183	203	30	-1094

Table.3: Comparison of Cutter Stress in the Three Ways between Edge and Shank

Force	Cutter stress at edge				
	Test (MPa)	FEM (MPa)	Error (%)	Analytic (MPa)	Error (%)
50	116.16	121.66	4.52	112.72	3.05
100	238.14	243.32	2.13	225.44	5.63
150	357.10	364.98	2.16	338.16	5.60
200	472.51	486.64	2.91	450.88	4.80
250	595.03	608.30	2.18	563.60	5.58
300	721.98	729.96	1.09	676.32	6.75
350	843.82	851.63	0.92	789.04	6.94
400	965.67	973.29	0.78	901.76	7.09
Average error (%)			2.09		5.68
Force	**Cutter stress on shank**				
	Test (MPa)	**FEM (MPa)**	**Error (%)**	**Analytic (MPa)**	**Error (%)**
50	14.36	12.76	12.52	13.81	3.94
100	26.34	25.52	3.21	28.80	8.53
150	40.14	38.28	4.85	43.20	7.08
200	52.25	51.04	2.36	57.60	9.29
250	66.06	63.80	3.53	72.00	8.26
300	79.60	76.57	3.96	86.40	7.87
350	92.85	89.33	3.94	100.80	7.89
400	104.49	102.09	2.35	115.20	9.30
Average error (%)			4.59		7.77

The error between FEM, experiments and analytical are shown in the Table 3. The reason is followings:

Plane stress problem is considered in experiment. Three-dimensional stress is considered in FEM and in analytical method only normal stress in the cross section is considered for shank stress and three normal stresses and two shear stresses are considered for cutter edge stresses. Although the cutter is firmly constrained and the values of stress are zeros in FEM and analytical method, stress and deflection of constrained part in experiment may be small value. The elemental cutting forces of *x*-, *y*- and *z*-directions are used in FEM and analytical method and one-directional point load is used in experiment. In FEM, the mesh density, cutter models and boundary conditions can affect the error. In analytical method, cutters are represented as cantilevered beam and cross sectional diameter of fluted part is 0.9 of shank diameter of cutter. Human error can occur when values from indicators are reading and calculating.

CONCLUSION

This paper shows the model and simulation of stress obtained by FEM and analytical method compared with the experimental results.

1. A theoretical model of cutting force and stress of tool has been established. The correct prediction of stress has been conducted according to the machining parameters.
2. The simulation of stress of tool has been performed by FEM. The stress and deflection has been obtained and compared with the theoretical analysis.
3. The stress of tool was measured with electrical-resistance strain gage. The results are used to verify to theoretical analysis.

ACKNOWLEDGEMENTS

The authors gratefully acknowledge the support of the “National Natural Science Fund” (51105025) and “International Science & Technology Cooperation Program of China” (2013DFB70110).

REFERENCES

Kurt A., 2009. Modeling of the Cutting Tool Stresses in Machining of Inconel 718 using Artificial Neural Networks. *Expert Systems with Applications*, 36 (6), 9645–9657.

Tsai C. L., 2007. Analysis and prediction of cutting forces in end milling by means of a geometrical model. *International Journal of Advance Manufacture Technology*, 31, 888–896.

Budak E., Altintas Y., Armarego, E., 2007. Prediction of milling force coefficients from orthogonal cutting data. *Transactions of the ASME*, 118, 216–224.

Jemal G., 1992.*Stress analysis of metal cutting tool*, Thesis (PhD). The University of British Columbi*a*.

Zhou J. M., Andreson M. and Ståhl J. E., 1997.Cutting tool fracture prediction and strength evaluation by stress identification, Part I: stress model. *International Journal of Machine Tools & Manufacture.* 12(37), 1691–1714.

Kops L., Vo D.T., 1990. Determination of the equivalent diameter of an end mill based on its compliance. *CIRP Annals Manufacturing Technology*, 39, 93–96.

Kumar M. P., Mohan B., Rajadurai A., Dinakar B. R., 2003. Modeling and analysis of orthogonal cutting of steel using FEM. *Proceedings of International Conference on Mechanical Engineering*. 12

Rendler N. J., Vigness I., 1996. Hole-drilling strain-gage method of measuring residual stresses. *Experimental Mechanics*. 6, 577–586.

Wu Q., Zhang Y. D., Zhang H. W., 2009. Corner-milling of thin walled cavities on aeronautical components. *Chinese Journal of Aeronautics*. 22, 677–684.

AUTHORS BIOGRAPHY

Wu Qiong, now is a lecturer in Beihang university. He has obtained Ph.D. in 2009 and finished Postdoctoral in 2011 at the School of Mechanical Engineering and Automation in Beihang University, China. His main research interest includes analysis and simulation of manufacturing and design as well as FEM.

Li Da Peng, now read for Master Degree at School of Mechanical Engineering and Automation in Beihang University. His main research interest in simulation of manufacturing process.